

Software Trigger Algorithms to Search for Magnetic Monopoles with the NOA Far Detector

This content has been downloaded from IOPscience. Please scroll down to see the full text.

2014 J. Phys.: Conf. Ser. 513 012039

(<http://iopscience.iop.org/1742-6596/513/1/012039>)

View [the table of contents for this issue](#), or go to the [journal homepage](#) for more

Download details:

IP Address: 131.225.23.169

This content was downloaded on 26/11/2014 at 20:52

Please note that [terms and conditions apply](#).

Software Trigger Algorithms to Search for Magnetic Monopoles with the NO ν A Far Detector

Z. Wang¹, E. Dukes¹, R. Ehrlich¹, M. Frank¹, C. Group^{1,2}, A. Norman²

¹ University of Virginia, Department of Physics, 382 McCormick Rd, Charlottesville, VA 22904, USA

² Fermi National Accelerator Laboratory, P.O. Box 500, Batavia, IL 60510, USA

E-mail: zw4vm@virginia.edu

Abstract. The NO ν A far detector, due to its surface proximity, large size, good timing resolution, large energy dynamic range, and continuous readout, is sensitive to the detection of magnetic monopoles over a large range of velocities and masses. In order to record candidate magnetic monopole events with high efficiency we have designed a software-based trigger to make decisions based on the data recorded by the detector. The decisions must be fast, have high efficiency, and a large rejection factor for the over 100,000 cosmic rays that course through the detector every second. In this paper we briefly describe the simulation of magnetic monopoles, including the detector response, and then discuss the algorithms applied to identify magnetic monopole candidates. We also present the results of trigger efficiency and purity tests using simulated samples of magnetic monopoles with overlaid cosmic backgrounds and electronic noise.

1. Introduction

The hypothetical magnetic monopole has been searched for since Dirac [1] put forward the idea of stable particles carrying magnetic charge. It is generally believed that the energy loss of magnetic monopole through matter only depends on its velocity, once the magnetic and electric charge it is carrying are specified. The magnetic monopole we discuss carries one Dirac charge ($g_D = \frac{\alpha}{2}e$) and no electric charge, and is usually referred as a Dirac monopole. Though many efforts have been made to search for magnetic monopoles, no solid evidence has been found to prove their existence.

Magnetic monopoles should deposit energy in matter in increasing amounts as their speed increases, monopoles with $\beta \gtrsim 0.01$ depositing about one to four orders of magnitude more energy than a minimum-ionizing particle (MIP). For such monopoles the large energy deposit along their track provides a spectacular signature that separates them from potential backgrounds. On the other hand, slower monopoles deposit less energy with decreasing β until at around $\beta = 10^{-5}$ to $\beta = 10^{-4}$ their energy deposit is roughly the the same as a MIP, making them more difficult to identify. This is why the sensitivity of previous searches decreases with decreasing β , and disappears altogether at $\beta \lesssim 10^{-5}$, as shown in Fig. 1. In addition, for a surface detector such as the NO ν A far detector, there is a large cosmic-ray flux that needs to be rejected as a $\beta = 10^{-4}$ monopole takes 0.5 ms to cross the detector transversely, and even longer from front to back. The challenge, in such a large time window, is to pick out the hits caused by the monopole among the many spurious hits caused by cosmic-ray backgrounds and electronic



noise. Trigger strategies hence naturally fall into two regimes: the ‘fast’ regime of $\beta \gtrsim 10^{-2}$, where the distinguishing feature is the spectacularly large energy deposit along the track, and the ‘slow’ regime of $\beta \lesssim 10^{-2}$, where the signature is a large transit time across the NO ν A far detector.

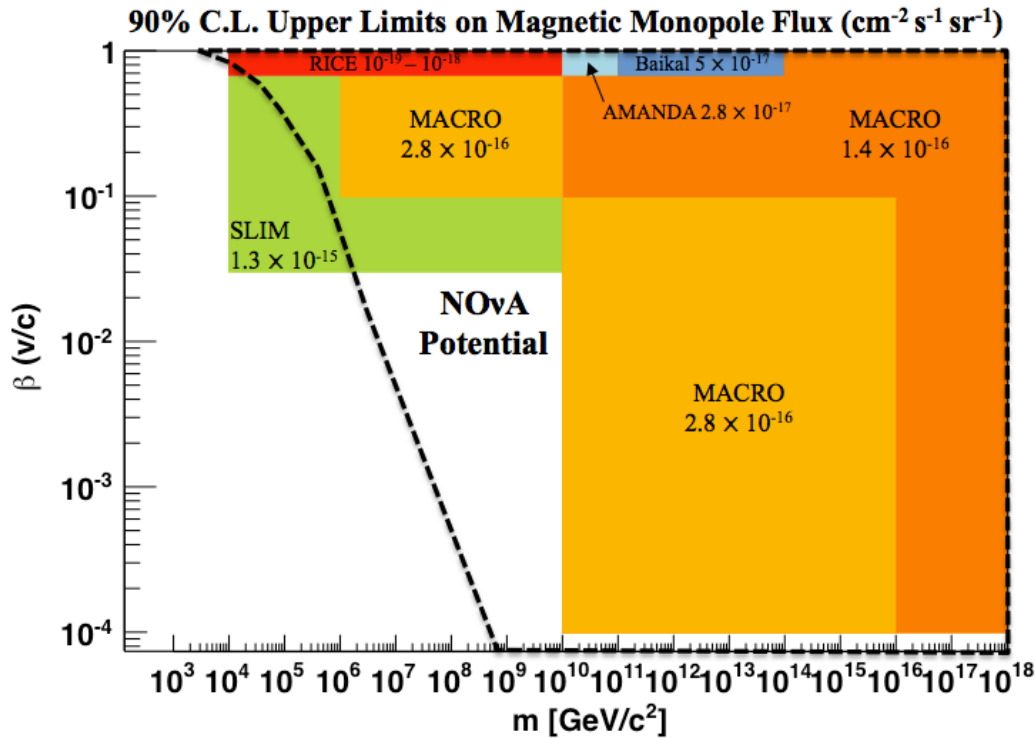


Figure 1: A visual summary of magnetic monopole flux upper limits from MACRO [2], SLIM [3], RICE [4], AMANDA [5] and BAIKAL [6] in the phase space of monopole mass and velocity, where inside the dashed line is the expected NO ν A sensitive region[7].

2. The NO ν A Detector and Data Readout

The NO ν A far detector has a mass of 14k-ton and is located near the surface in northern Minnesota, USA. When completed it will contain 340,064 liquid scintillator-filled detection cells with embedded wave-shifting fibers read out at both ends by avalanche photodiodes. Each cell has a $3.8 \times 5.9 \text{ cm}^2$ cross section, and is 15.5 m long. The cells are arranged in alternating x and y planes, and the entire detector is 59.5 m long. The partially fabricated far detector is being commissioned. Results described here are based mainly on simulations and are preliminary.

The NO ν A far detector is continuously live, not just during the beam spill in which neutrinos are sent to it from Fermilab. The front-end readout continuously digitizes the data in each cell in 500 ns increments, sending out zero-suppressed data to the data acquisition system (DAQ). The data, in 5 ms time windows (referred to as millislices), is sent to a large computing farm. All of the data from the detector is stored in the farm for about ten seconds, a time that is needed to (1) allow the accelerator spill time information to propagate from Fermilab to the far detector, and (2) allow software data-based triggers time to make their decisions. In this period, roughly 500 cosmic-ray muons will traverse the detector. Hence, the track-finding algorithm must reconstruct a track within 20 ms on average. Monte Carlo tests of the DAQ and the tracking algorithm described below have shown that it meets this requirement. Events in NO ν A

are not interactions, such as might be recorded in a collider or fixed-target detector, but rather time slices, which can be as small as a $50 \mu\text{s}$, called a microslice, or as large as the 5 ms millislice. Only a few percent of the raw data produced by the detector can be sent to permanent storage. The raw data is dominated by cosmic rays and detector noise.

3. Magnetic Monopole and Cosmic Ray Background Simulation

The simulation of the response of the NO ν A far detector to magnetic monopoles is done by GEANT4 [8]. The time and energy response of a single cell's front-end electronics to monopoles of different velocities has been simulated (assuming no noise) and is shown in Fig. 2. This illustrates the very different detector response over the range of monopole velocities of interest. The energy deposit of any charged particle to a cell is characterized by the digitized output of the corresponding channel, in the unit of ADC counts.

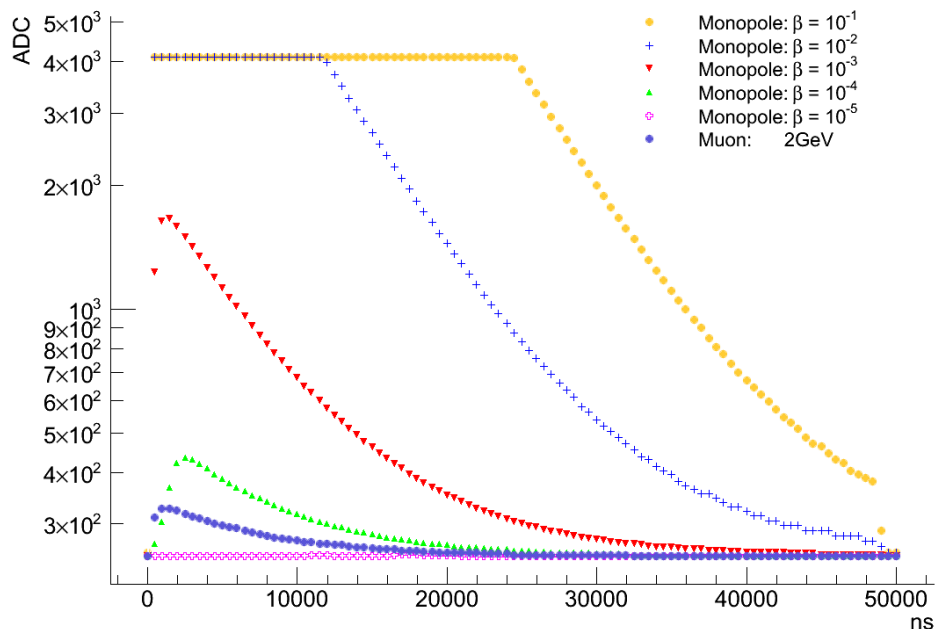


Figure 2: The electronics response of the front-end electronics for monopoles crossing a detector cell. Fast (high β) monopoles are characterized by large energy deposits, which can reach the maximum ADC value. For comparison, note that a minimum ionizing particle with the same path length will on average deposit about 12 MeV in a cell.

Cosmic ray events are simulated using the CRY [9] code package with a very detailed GEANT4 model of the detector response. Monopoles are generated uniformly over all solid angles. Monte Carlo cosmic ray events are overlaid with the magnetic monopoles, as shown in Fig. 3. If a monopole and a cosmic ray cross a cell simultaneously, the simulation correctly models the time dependence of the cell response to the energy deposited by the two particles.

4. Fast Monopole Trigger

As mentioned above, fast monopoles ($\beta \gtrsim 10^{-2}$) are identifiable by their high energy deposition within a limited time window: $50 \mu\text{s}$, called a microslice, in which the monopole track is completely contained. A monopole produces a well defined linear track with a large numbers

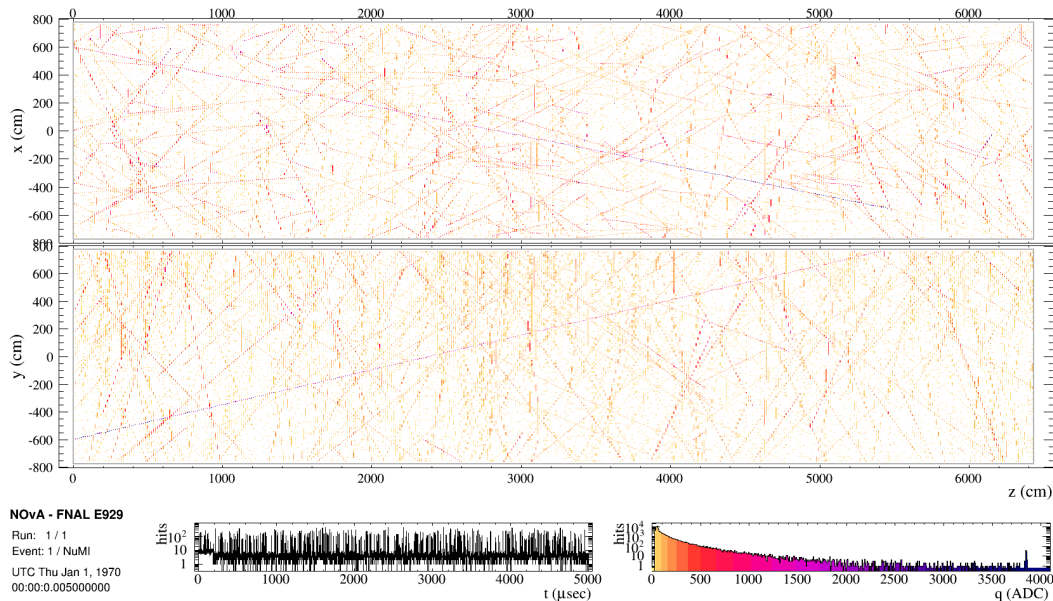


Figure 3: Simulation of a magnetic monopole with mass = $10^{16} GeV/c^2$ and $\beta = 10^{-3}$ in the NOνA far detector, within a 5 ms millislice, with overlaid cosmic rays and detector noise. The monopole track is easily separable from cosmic ray background due to timing and pulse height information. The top(bottom) part of the top figure shows the energy deposited in the vertical(horizontal) cells. The bottom two plots show the time of arrival with the millislice of the hit cells (left) and the energy spectrum of the hit cells (right).

of channels at or near the maximum possible value of the digitized output(4096 ADC counts, referred to as “saturation”). A simple total energy based trigger has been found to have good efficiency with sufficient cosmic-ray background rejection to keep it within the allowed trigger bandwidth. The fast trigger algorithm requires: (1) a minimum number of cells to have an energy exceeding a high threshold, well beyond that of the dominant cosmic-ray muon background; (2) an average energy of hit cells to be greater than a second threshold; and (3) a certain number of hit cells to be near the edge of the detector. The last requirement only decreases the trigger rate by roughly a factor of two.

The efficiency and rejection of the fast monopole trigger has been simulated by overlaying isotropic fast ($\beta \gtrsim 0.01$) monopoles onto cosmic rays and noise hits. The trigger efficiency as a function of both thresholds described above is shown in Fig. 4(a). It is very high over a large range of both thresholds. The cosmic-ray rejection, in terms of the trigger rate, is shown in Fig. 4(b), again as a function of the two trigger thresholds. The target rate is about 1 Hz, which is satisfied by a large range of both thresholds. The final determination of the two thresholds depends on the real detector noise rate, the cosmic-ray background rate, and the trigger bandwidth budget assigned to the fast monopole trigger.

5. Slow Monopole Trigger

The slow monopole trigger must be more sophisticated as the number of cosmic-ray background events is much larger due to the larger time window, and the lower energy deposit of the slower monopoles precludes using the simple total energy algorithms employed by the fast monopole trigger. The scope of the problem is evident in Fig. 3, which shows a $\beta = 10^{-3}$ monopole in a millislice time window. Note that a very slow monopole track might produce only a single cell hit within any one microslice.

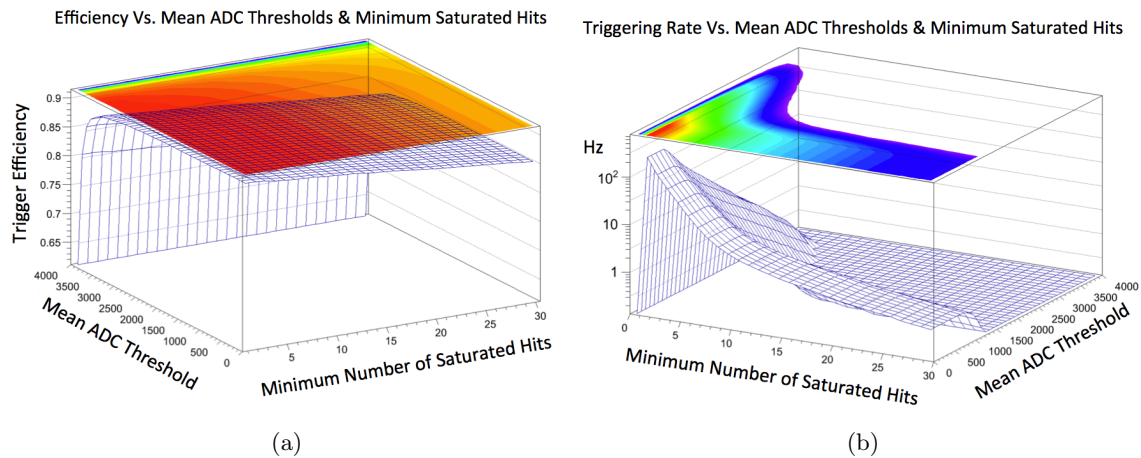


Figure 4: (a) The fast monopole trigger efficiency as a function of both energy thresholds. (b) The simulated trigger rate of cosmic-ray backgrounds with the fast monopole trigger, again as a function of both energy thresholds..

Reconstructing all of the tracks within the entire millislice to find the one slow track consistent with a $\beta < 10^{-2}$ monopole takes a prohibitive amount of computer time. A different algorithm is used, which relies on the fact that the cosmic-ray background consists largely of fast muons which traverse the detector within a microslic. The combinatorics (pairs of hits) are much reduced by first finding the cosmic-ray muons microslic-by-microslic, and eliminating all cell hits associated with them. This leaves a millislice essentially devoid of cosmic-ray tracks, and left only with noise and the putative monopole candidate.

To find the cosmic-ray background tracks we employ a global pattern recognition method based on a 2D Hough transform. Pairs of cell hits are used to find track stubs whose distance of closest approach (DOCA) and angle ($\cos\psi$) with respect to the z-axis of the NO ν A coordinate system are determined. The detector is divided into ten regions to minimize the combinatoric burden. If there are more than a certain minimum number of track stubs with identical DOCA and $\cos\psi$ values, then we have a monopole candidate.

Once all the cosmic-ray background tracks within the millislice have been found, and their hits subtracted out, another Hough transform track finding algorithm is employed: this time over all hits remaining in the entire millislice. This algorithm uses the similar geometry parameters like DOCA and $\cos\psi$ as before, along with one additional parameter: the speed of the track stub, that is the distance between the two points divided by the time separation. Actually the inverse of the speed is used, v_{pro} , because although the space difference between cell hits is perfectly well determined, the time difference sometimes is not, and can be zero.

This entire module is now under test with the latest cosmic data we have collected.

6. Conclusions

Two monopole trigger algorithms have been developed: one for fast monopoles ($\beta \gtrsim 10^{-2}$), another for slow ($\beta \lesssim 10^{-2}$) monopoles. Preliminary Monte Carlo studies promise a high efficiency with good background rejection for the fast monopole trigger. The challenging slow monopole trigger is still under tuning based on the cosmic data we are currently taking. The overlap region between the two algorithms remains to be determined, and is somewhat dependent on detector performance parameters — noise, hot channel counts, etc. — that are presently not well known.

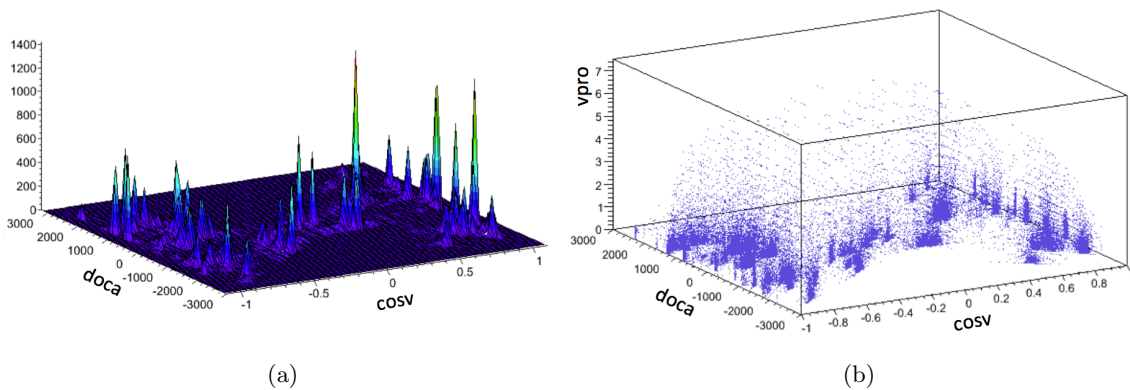


Figure 5: (a) The population of the 2D Hough space, with each peak representing a cosmic-ray muon track. (b) The 3D Hough space, populated again by cosmic-ray muons: a monopole track would present itself as a cluster of hits well above the points shown in the figure.

References

- [1] P.A.M. Dirac, Proc. Roy. Soc. Lond., A133, 60 (1931).
- [2] M. Ambrosio *et al.*, Eur. Phys. J. C25, 511 (2002).
- [3] S. Balestra *et al.*, Eur. Phys. J. C55, 57 (2008).
- [4] D.P. Hogan *et al.*, Phys. Rev. D78, 075031 (2008).
- [5] R. Abbasi *et al.*, Eur. Phys. J. C69, 361 (2010).
- [6] V. Aynutdinov *et al.*, Astropart. Phys. 29, 366 (2008).
- [7] This curve is the minimum kinetic energy required for the magnetic monopole to reach the NO ν A detector, as a function of the monopole mass. The calculation is done with approximated energy loss of the monopole passing through the atmosphere and the overburden on the top of the detector.
- [8] We use GEANT4.9.6 with G4mplIonisation.
- [9] C. Hagmann, D. Lange, J. Verbeke, and D. Wright, UCRL-TM-229453 (2012).